PAPER REF: 2760

INSTRUMENTATION OF A RACING BICYCLE FOR OUTDOOR FIELD TESTING AND EVALUATION OF THE CYCLIST'S COMFORT PERCEPTION

Joachim Vanwalleghem[1*], Frederik Mortier[1], Ives De Baere[1], Mia Loccufier[2] and Wim Van Paepegem[1]
[1]Department of Materials Science and Engineering, Ghent University, Faculty of Engineering and Architecture, Belgium
[2]Department of Electrical Energy, Systems and Automation, Ghent University, Faculty of Engineering and Architecture, Belgium
[*] Email: Joachim.Vanwalleghem@UGent.be

ABSTRACT

High frame stiffness is one of the most important parameters a racing bicycle should fulfil, it shows advantages in steering stability and a smaller amount of pedalling power is lost due to frame deflection. On the contrary, increased stiffness may attenuate the shock absorption ability of the frame and consequently leading to lack of comfort for the cyclist. This work proposes the absorbed power criterion to assess the cyclist’s comfort at in-situ conditions and therefore the racing bicycle must be instrumented with sensors which measure the contact force and -velocity. This paper describes how all sensors are designed, calibrated and tested for their good functioning. Initial outdoor field tests have shown that all sensors work properly and that the absorbed power method can be used for future work regarding human comfort and how it is affected by parameters such as tyre pressure or cycling position.

Keywords: human comfort, field testing, cycling, absorbed power, sensor design

INTRODUCTION

Bicycles, and especially racing bicycles, have evolved from simple frame constructions up to state of the art technology. To achieve this, effort is mostly invested in increasing the stiffness of the bicycle frame through modifications in frame geometry and frame material. Carbon fibre reinforced epoxy material is found to suit for this application because both low weight and high stiffness are of major concern for the cyclist’s performance. Unfortunately, the cyclist perceives a reduced feeling of comfort with this new type of bicycle frames. A wide variety of shock absorption improvements has been introduced by bicycle manufacturers, such as rubber frame inserts, high damping frame materials instead of full carbon frames and adding flexible zones into the frame. From a subjective point of view these improvements may lead to comfort gain, but still the bicycle designer cannot quantify the effect it has onto bicycle dynamics and the cyclist’s comfort perception. Comfort improvement is not new in other industries, e.g. automotive, and therefore different comfort evaluation criteria have been developed. One method is the whole-body and hand-arm vibration method (ISO2631-1997; ISO5349-1,2001; BS6841, 1987) which relates acceleration levels at the contact points between man and machine to human comfort. The second evaluation criteria is the absorbed power method (Pradko et. al., 1967; Wilson, 2004), this method is more sophisticated concerning machine sensor instrumentation but gives more information on the man-machine interface and corresponding comfort level (Mortier, 2010). Absorbed power is a measure for the vibration level at the human being in terms of contact velocity $v(t)$ and contact force $F(t)$ and is defined as:

$$\overline{P_{Abs}} = \frac{1}{T}\int_0^T F(t) \cdot v(t)dt \qquad (1)$$

So far, the absorbed power method is mainly used in laboratory environment since this facilitates the sensor instrumentation and corresponding data acquisition (Mansfield and Griffin, 1998; Lundström et. al., 1998; Pradko et. al, 1967). The challenge of this study is to equip a bicycle with all necessary sensors and data readout devices for in-situ measurements. This test-setup is necessary because the cyclist's comfort is best evaluated during outdoor conditions. This leans close to a normal cycling condition and also data is gathered from actual road pavement data. The latter excites the bicycle near the two wheels and thus is responsible for the cyclist's comfort perception.

This paper describes the bicycle sensor instrumentation for the cyclist's comfort evaluation during cycling by means of the absorbed power method. This includes the design of force- and velocity sensors near the contact points between the bicycle and cyclist: the handlebar, the saddle and the pedals. Human comfort is evaluated only at the steer and the handlebar because it is believed that vibrations at these contact points are most detrimental for cyclist. Force- and velocity measurements at the pedal are used for measuring pedal force patterns and can be used for the cyclist's pedalling technique improvement.

Sensor design is described from conceptual idea to calibration and final implementation and testing. In the end some initial field tests are performed which show the correct functioning of all sensors independently and whether or not the absorbed power method can be applied successfully.

DESIGN CONCEPT

Force sensor design

The challenging task in measuring forces at the contact points is that (i) bicycle components should maintain their original geometry and functioning as much as possible, (ii) the force sensors should be modular meaning they fit any racing bicycle, (iii) in-situ measurements require a robust design and (iv) the force measurements must be accurate and repeatable. The final design of the transducer will be a compromise of all these, but demands at least a good load sensitivity in a modular concept. The concept of measuring force at all contact points is based on the strain gradients occurring in a cantilever beam when a load is applied on it. This concept is chosen because of its high strain sensitivity: even low load amplitudes give rise to a high bending strain. Fig. 1 shows how the strain gauges are mounted onto the cantilever beam. The Wheatstone bridge configuration is somewhat different compared to common full bridge configurations because the output signal is proportional to the difference in bending moment measured at two locations *1* and *2* on the cantilever beam. The strain due to the bending moment is measured at location *1* and *2* at a distance b from each other, measuring respectively a high and low bending strain. Thus, the output voltage V/V_{ex} is proportional to the slope of the bending moment line which is in turn independent of the position c of the force and proportional to $F \cdot b$. This principle is of big interest when force is measured at the handlebar: even if the position of the hands changes along the handlebar under the same force amplitude, there is no effect on the output signal.

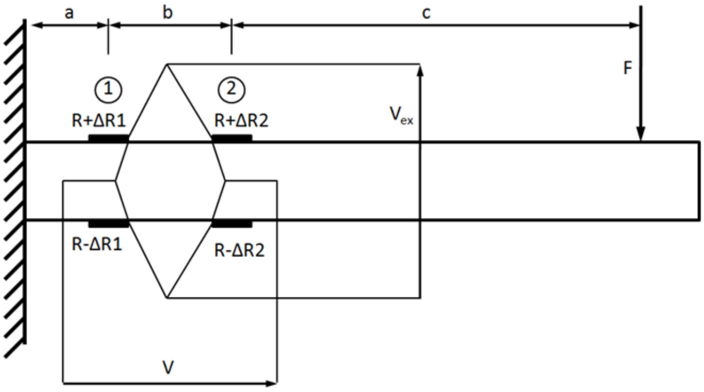

Fig. 1 Strain gauge configuration used for force sensor design

The output signal from the Wheatstone bridge configuration is [Mortier, 2010]:

$$\frac{V}{V_{ex}} = \frac{GF}{2 \cdot W \cdot E} F \cdot b \quad [\frac{mV}{V}] \tag{2}$$

which clearly shows that the output voltage is only dependent on the force *F*, the gauge factor *GF*, the section modulus of the beam *W*, the elasticity modulus of the beam *E* and the distance *b* between the two pair of strain gauges at one side of the beam.

Velocity form integrating acceleration signal

Measuring contact velocity requires a less complicated sensor design since velocity results from integrating the acceleration signal. The only difficulty which comes up in the integrating process is that drift may arise in the velocity signal due to a DC value in the acceleration signal. The design and calibration section takes a closer look on how this problem is solved.

Crank position and -velocity measurement

The crank position is measured based on the encoder principle, shown in Fig. 2 and Fig. 3. The front chain sprocket, in combination with two inductive sensors (*A* and *B*) and one reference point *C*, generates pulses from which the position, direction and velocity can be found. The main advantage of this configuration is that it excels in simplicity, accuracy and robustness. The added weight to the bicycle is reduced to a minimum and it hardly requires modifications to the bicycle. This is in contrast with other systems found in literature which require large modifications to the crank mechanism (Alvarez and Vinyolas, 1996; Drouet et. al., 2008), or only can be used for indoor testing (Tielert, et. al., 2008; Bolourchi and Hull, 1985; Reiser et. al., 2003]

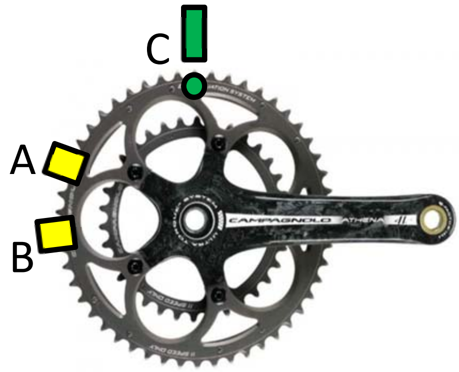

Fig. 2 Concept for registration of crank position -and velocity

Fig. 3 Practical realization of crank position -and velocity

DESIGN AND CALIBRATION OF FORCE- AND VELOCITY SENSORS

Saddle force

Force measurements at the saddle are only possible through mounting a force gauge in between the saddle and the seat tube. The C-shaped part shown in Fig. 4 allows for force measurement in two orthogonal directions, thus both the horizontal and vertical force component at the saddle can be measured. The horizontal and standing side of the insert are foreseen of each a full Wheatstone bridge configuration (as in Fig. 1) and measure respectively the vertical and horizontal saddle force component. Both components are well uncoupled, this is verified numerically through finite element analysis as well from calibration tests shown in Fig. 5. Equation (3) and (4) give the sensitivity of the Wheatstone bridges for both the horizontal and vertical saddle force component, this confirms (i) the linear relation between applied load and output voltage and (ii) both force components are well uncoupled

Fig. 4 Position of saddle force gauge in between the saddle and the seat tube

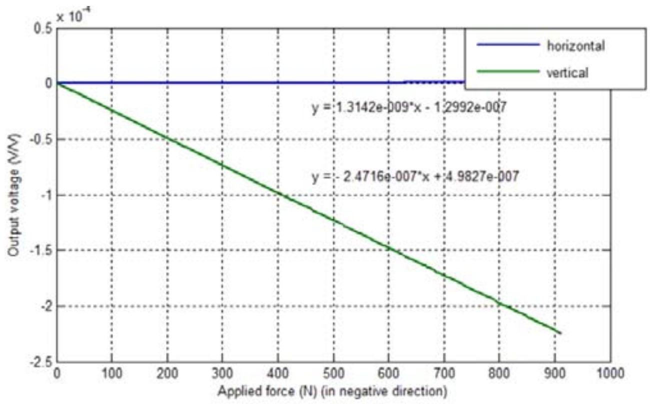

Fig. 5 Sensitivity curve of saddle force gauge: horizontal and vertical component are uncoupled

$$F_{hor} = 4225.353 \cdot \frac{V_{hor}}{V_{ex}} + 22.463 \cdot \frac{V_{vert}}{V_{ex}} \; [\frac{N}{\frac{mV}{V}}] \qquad (3)$$

$$F_{vert} = 4045.733 \cdot \frac{V_{vert}}{V_{ex}} - 21.278 \cdot \frac{V_{hor}}{V_{ex}} \; [\frac{N}{\frac{mV}{V}}] \qquad (4)$$

Handlebar force

Force measurements at the handlebar are done at both the left and right hand side which brings in total twice two pair of full bridge configurations or 16 strain gauges, as illustrated at Fig. 6. The stem holds the handlebar in the middle and should therefore decouple the left from the right hand side of the steer, see Fig. 6. Unfortunately, from initial calibration tests followed that the left and right hand side are not uncoupled. Two effects have found to be responsible for this. When tightening the bolts which clamp the stem onto the handlebar, stress is induced in the hollow section of the handlebar which then causes an output signal at all Wheatstone bridges. A second effect is called ‘zero offset’: when a force on the handlebar is applied and released again, the signal from the Wheatstone bridges does not return to their initial (unloaded) value. This effect is due to slippage of the handlebar in the stem and causes an offset in the range of 30% to 40% of the loading. Previous issues can be solved by having a solid section at the region where the stem is clamped onto the handlebar; the curved ends of the handlebar are then glued to the insert. Fig. 7 shows the technical drawing of the redesigned handlebar. Calibration results, as given by Equations (5)-(8), show perfect uncoupling among all Wheatstone bridges. Besides this, the zero offset is removed also.

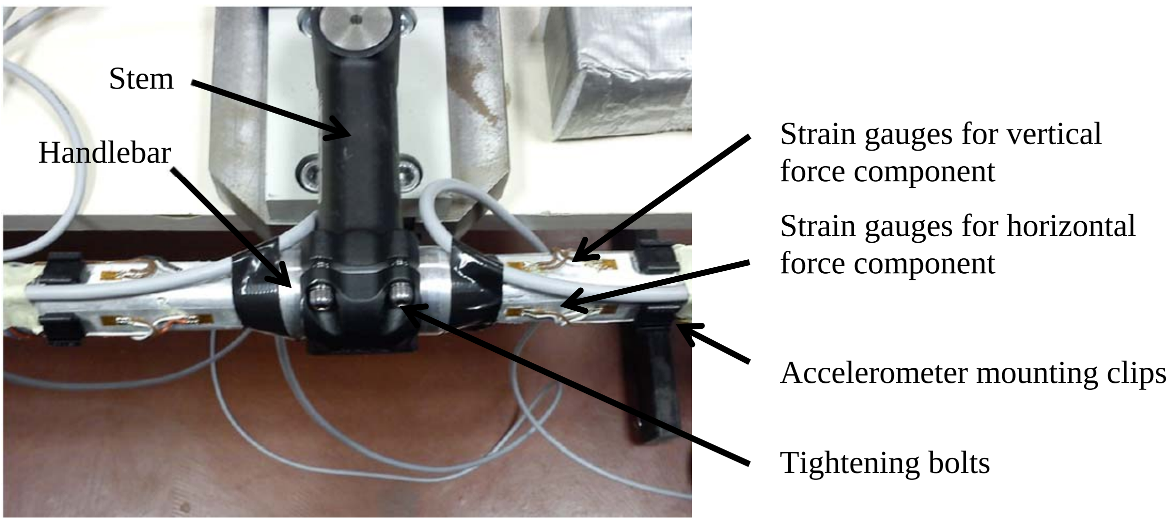

Fig. 6 Strain gauge configuration at handlebar

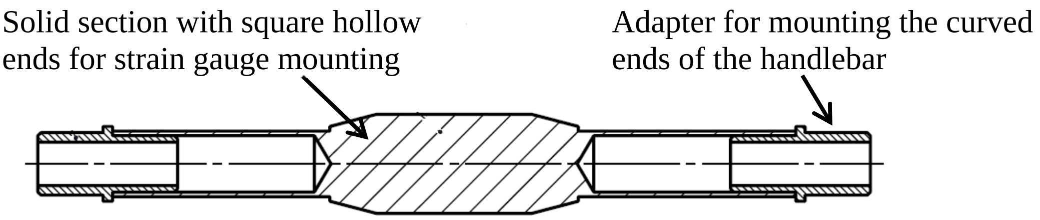

Fig. 7 Redesign of handlebar

Left hand side:

$$F_{vert} = 1580 \cdot \frac{V_{vert}}{V_{ex}} \left[\frac{N}{\frac{mV}{V}}\right] \tag{5}$$

$$F_{hor} = 1602.3 \cdot \frac{V_{hor}}{V_{ex}} \left[\frac{N}{\frac{mV}{V}}\right] \tag{6}$$

$$F_{vert} = 1495.3 \cdot \frac{V_{vert}}{V_{ex}} \; [\frac{N}{\frac{mV}{V}}] \quad (7)$$

Right hand side:

$$F_{hor} = 1454.3 \cdot \frac{V_{hor}}{V_{ex}} \; [\frac{N}{\frac{mV}{V}}] \quad (8)$$

As with the saddle force gauge, this handlebar design allows to measure all force components without large modifications to the bicycle. Other designs found from literature show some limitations regarding the number of force components which can be measured (Champoux et. al., 20070, or the original handlebar should be replaced by a simplified handlebar (Champoux et. al., 2004) to sustain the high level of forces.

Pedal force

Pedal force acquisition systems are commercially available but often show shortcomings such as low sample rate and the fact that the pedal position is not registered simultaneously (Barratt, 2008). Therefore different measurement systems and handmade pedal designs have been proposed (Reiser et. al., 2003; Drouet et. al., 2008; Tielert et. al., 2008; Alvarez and Vinyolas, 1996). All of them have shown to work, but some require own pedal design and thus no commercial available pedal can be used, require modifications to the crank or only can be used for indoor testing. Because of this it is necessary to design a measurement system which does fulfils these issues. During the design process revealed that the main restriction is the rotating crank which makes data transmission from sensor to the storage unit difficult. Eventually, it is chosen to start from a standard available pedal on which two pair of Wheatstone bridges are placed (see Fig. 8). Further on, a data acquisition module is mounted onto the crank which sends the sensor data to the storage unit through Bluetooth connection as shown at Fig. 9. As with all previous load cells, calibration is successful, as shown by Equations (9) and (10) which show how the force in both orthogonal directions, F_1 and F_2, varies linearly with the Wheatstone bridge output voltage $\frac{V}{V_{ex}}$ $[\frac{mV}{V}]$.

Fig. 8 Strain gauge configuration at pedal

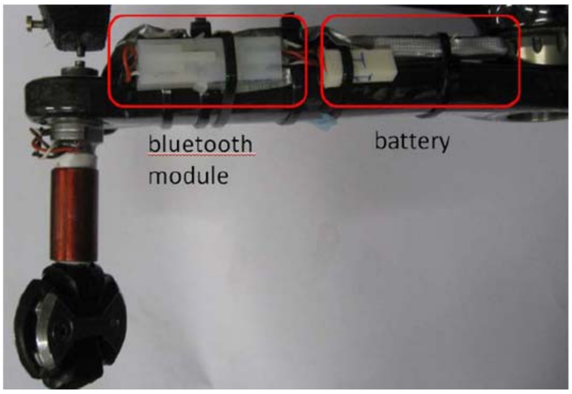

Fig. 9 Local data acquisition and Bluetooth transmission of pedal force

$$F_1 = 1432 \cdot \frac{V_1}{V_{ex}} \; [\frac{N}{\frac{mV}{V}}] \quad (9)$$

$$F_2 = 1448.7 \cdot \frac{V_2}{V_{ex}} \; [\frac{N}{\frac{mV}{V}}] \quad (10)$$

Integrating acceleration to velocity

Integrating acceleration to velocity inevitable gives a drifting velocity signal. This drift can be removed through high-pass filtering the acceleration signal, but this causes a time delay between the integrated acceleration signal and the real-time velocity signal. This issue has been observed in the calibration procedure. An electrodynamic shaker generates a random signal from which acceleration and velocity is measured. Acceleration is measured with an IEPE 100mV/g accelerometer and real-time velocity is measured with a laser Doppler vibrometer. Fig. 10 shows the real-time velocity- and integrated acceleration signal, the latter shows time delay and also amplitude does not fit perfectly. This phase shift should be removed because it could lead to errors in the calculation of the absorbed power at which force and velocity time signals are multiplied. Through filtering the force signal with an IIR low-pass filter with a cut-off frequency of 350Hz and 81 steps, the force signal is on the same time base as the integrated acceleration signal. Fig. 11 shows how this filter has a positive effect on the time-delay and amplitude level.

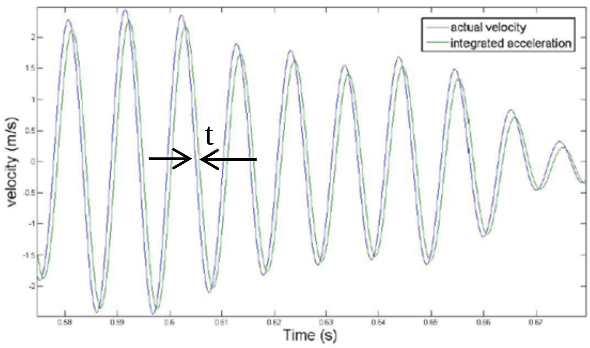

Fig. 10 Verification of integrated acceleration signal with real time velocity signal: time delay *t* between both

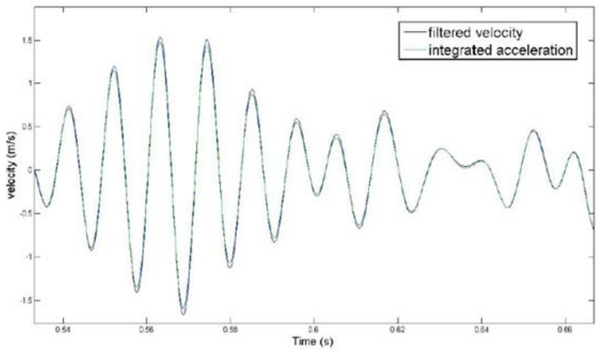

Fig. 11 Integrated acceleration signal fits the real time velocity signal after low pass filtering

Data acquisition

Acquiring all signals from the sensors on the bicycle is done through National Instruments (NI) DAQ modules and corresponding LabView software. Data is sampled at a 1652Hz sample rate which is the minimum sample rate of NI modules and data is transmitted to the laptop using a USB cable. Power supply for the chassis is foreseen by a 12VDC lead-acid battery with a 2.2Ah capacity. All previous items are placed in a rucksack, giving a weight of 9.6kg.

RESULTS FROM FIELD TESTING

From previous calibration tests it could be concluded that all sensor work individually. Initial field tests are performed to check whether or not all these sensors function during outdoor conditions and if the absorbed power method can successfully be applied. All field tests are performed with a Museeuw Flax 5 (MF5) racing bicycle. The bicycle has a total mass of 11kg, instrumentation with acceleration- and force sensors included. The cyclist has a weight of 80kg.

Pedal force measurements

Pedal forces are measured at an asphalted road at a 38km/h cycling speed and 10km/h tail wind, the tyres were inflated to 9bar pressure and the crank length is 175mm. Fig. 12 shows a typical plot of the force pattern over one revolution, most force is generated in the first half whereas in the second half the weight of the leg rests on the pedal and consequently counteracts the upward motion. Combined with the crank velocity the instantaneous power is calculated, as shown in Fig. 13. It varies approximately sinusoidal with positive and negative peak values of 400W and -100W respectively. The average input power at one pedal is 100W, thus 200W input power in total is necessary for the cycling condition described above.

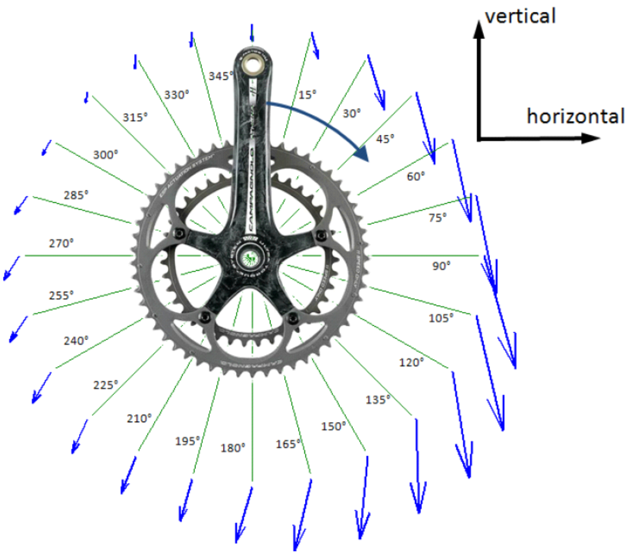

Fig. 12 Pedal force pattern during one crank revolution

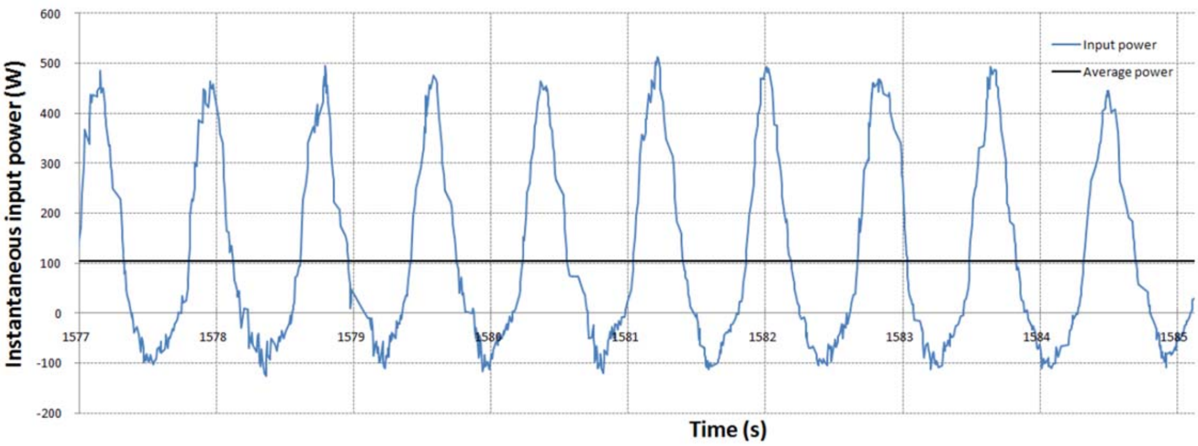

Fig. 13 Instantaneous power at pedal during a 30km/h ride at an asphalted road

Force distribution measurement at handlebar and saddle

The force sensor design at the handlebar and saddle is evaluated for its proper functioning through field tests at an asphalted road and at cobblestones road. Although force distribution data may not be reflected in a one to one relation to comfort perception, it can be used for bicycle frame design purposes. Fig. 14 and Fig. 15 show the vertical saddle force distribution for rides at an asphalted and cobblestones road respectively. The latter shows a slightly lower mean value but the spread is much higher, peaks up to 1400N are registered. Force distribution data at other contact points shows analogue results. These force measurements are found to be correct and can therefore be used for further analysis for the cyclist’s comfort evaluation through the absorbed power method.

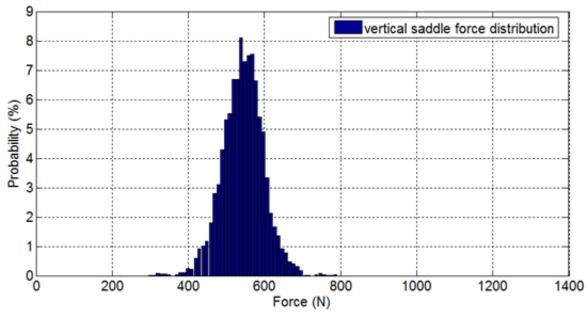

Fig. 14 Vertical saddle force distribution when cycling across an asphalted road

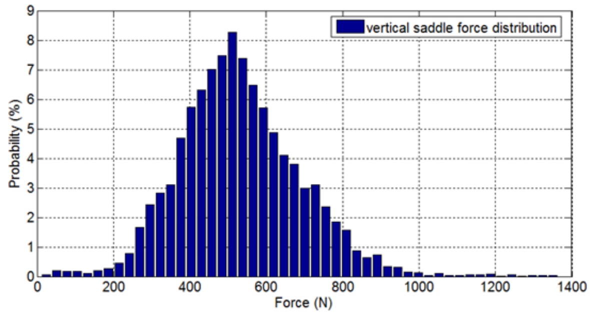

Fig. 15 Vertical saddle force distribution when cycling across a light cobblestones road

Absorbed power measurements

Two types of road pavement are used for comparison in comfort level, an asphalted road and a mild cobblestones road, each with a course of 180m and driven at 30km/h. Fig. 16 and Fig. 17 show the force- and velocity signal at the saddle in vertical direction, a detailed view of 0.5 seconds is depicted in Fig. 18 and Fig. 19 respectively. The force signal shows a time varying function around an average value, as observed also in Fig. 15, whereas the velocity signal is constantly varying around zero. Each peak in the velocity signal corresponds with a peak in the force signal as depicted in Fig. 18 and Fig. 19. The cumulated work, plotted in Fig. 20, is found from multiplying both force –and velocity signal as function of time, the average absorbed power value results from dividing the total work by the total time *T*. Fig. 20 depicts that the vertical saddle component shows a steep negative slope which is due to the high mean value for the vertical saddle force. Other components show also a linear decreasing function of cumulated work as function of time, but the slope is relatively small.

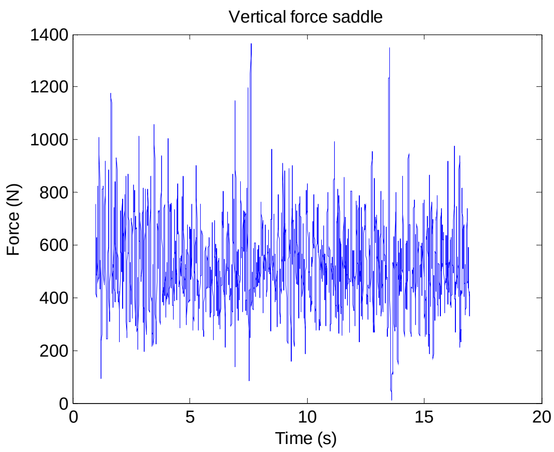

Fig. 16: Outdoor field test at cobblestones road: vertical saddle force as function of time

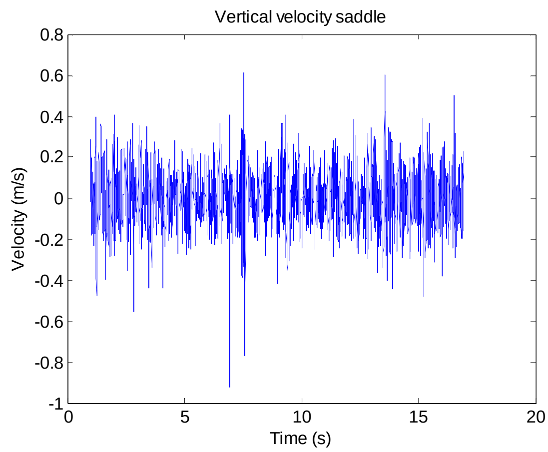

Fig. 17 Outdoor field test at a cobblestones road: vertical velocity at saddle as function of time

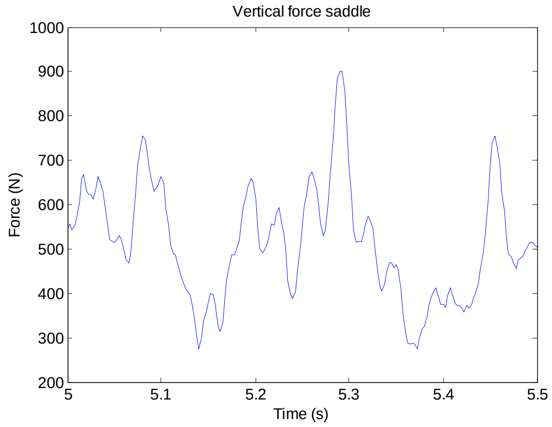

Fig. 18 Detailed view of Fig. 16

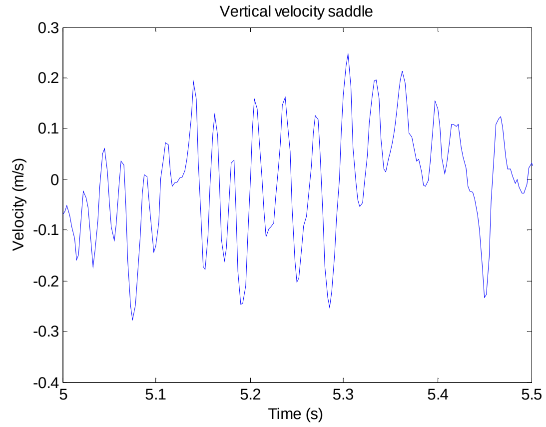

Fig. 19 Detailed view of Fig. 17

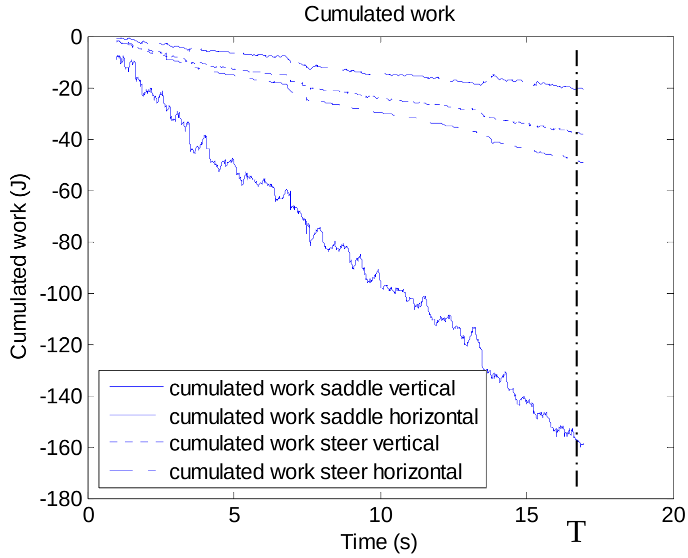

Fig. 20 Cumulated work at saddle and handlebar during field test at cobblestones road

This cobblestones ride gives a total absorbed power value of 21Watt, respectively 10.4Watt and 10.6Watt at the handlebar and the saddle respectively. If the same analysis is performed at an asphalted pavement, the total absorbed power is 1.2Watt which is significantly smaller than riding a cobblestones road. Additional tests are not executed yet because these tests only served to check for correct functioning of the bicycle instrumentation and data acquisition during outdoor conditions and whether or not the absorbed power correctly can be calculated. Based on these results, the test-setup has shown to function well and further can be used for supplementary test cases.

CONCLUSION

Evaluating human exposure to vibrations has already been investigated for many years but quantifying the feeling of comfort for the cyclist who's riding a rough pavement has not been assessed thoroughly so far. This paper proposes the absorbed power method to measure comfort during outdoor field tests. Both force- and velocity sensors are designed and installed onto the bicycle near the contact points of cyclist and bicycle, thus at the saddle, the handlebar and the pedal. Force is measured through strain gauge configurations and velocity is obtained from integrating acceleration data. These sensors hardly require modifications to the racing

bicycle so that the cyclist can maintain his normal cycling position. Besides this, the DAQ system, which is carried by the cyclist, is able to read and store data from 14 sensors simultaneously. Combining both the sensor design and the DAQ configuration allows for in-situ measurements during outdoor conditions. This enables to acquire data which is useful for both the cyclist and bicycle designer. The cyclist can improve his pedalling technique and the bicycle designer receives useful data of peak forces onto the frame and can evaluate whether or not his shock-absorption improvements to the bicycle have any effect.
Proper functioning of the instrumented bicycle is evaluated in preliminary outdoor field tests. These give an indication of force patterns at all contact points and if the absorbed power comfort evaluation criterion is calculated successfully. E.g. cycling at a cobblestones road with a 30km/h cycling speed gives a total absorbed power value of 21Watt. Further tests can give more information on how the cyclist's comfort changes with parameters as tyre pressure, frame material –and geometry, cycling position, etc.

REFERENCES

Alvarez G, Vinyolas, J. A new bicycle design for on-road measurements of cycling forces. Journal of applied biomechanics, 1996, 12, p. 130-142

Barrat P. SRM torque analysis of standing starts in track cycling. The engineering of sport 7 – vol.1, 2008, p.443-48

Bolourchi F, Hull M.L. Measurement of rider induced loads during simulated bicycling. International journal of sport biomechanics, 1985, 1, p. 308-329

BS 6841:1987, Guide to measurement and evaluation of human exposure to whole-body mechanical vibration and repeated shock.

Champoux Y, Richard S, Drouet J.M. Bicycle structural dynamics. Sound and Vibration, July 2007, p. 16-22

Champoux Y, Vittecoq P, Maltais, P, Auger E, Gauthier B. Measuring the dynamic structural load of an off-road bicycle frame. Experimental techniques, May/June 2004, p. 33-36

Drouet, J.M., Champoux Y, Dorel, S. Development of multi-platform instrumented force pedals for track cycling. The engineering of sport 7 – vol.1, p263-271

ISO 2631-1, Mechanical vibration and shock - evaluation of human exposure to whole-body vibration -- Part 1: General requirements, 1997.

ISO 5349-1:2001, Mechanical vibration -- Measurement and evaluation of human exposure to hand-transmitted vibration -- Part 1: General requirements.

Lundström R, Holmlund P, Lindberg L, Absorption of energy during vertical whole-body vibration exposure. Journal of biomechanics, 1998, 31, p. 317-326

Mansfield N.J, Griffing M.J. Effect of magnitude of vertical whole-body vibration on absorbed power for the seated human body. Journal of sound and vibration, 1998, 215, 4, p. 813-825

Mortier F. Evaluation of the dynamic behaviour of composite racing bicycles through outdoor field testing. Ghent University, Master's thesis 2010-2011

Pradko, F., R. Lee, and V. Kaluza, Theory of Human Vibration Response. Mechanical Engineering, 1967. 89, 2.

Reiser R.F., Peterson, M.L., Broker, J.P. Instrumented bicycle pedals for dynamic measurement of propulsive cycling loads. Sports engineering, 2003, 6, p. 41-48

Tielert R, Wehn N, Jaitner T, Volk R. Power measurement in cycling using inductive coupling of energy and data. The engineering of sport 7 – vol.1, 2008, p.397-403

Wilson D.G. Bicycling science 3rd-ed., 2004.